ESTIMATION OF SOURCE PARAMETERS FOR THE 2015 GORKHA EARTHQUAKE AFTERSHOCKS

Chintan Timsina* **Supervisor: Masumi YAMADA****
MEE16703 **Takumi HAYASHIDA*****

ABSTRACT

We analyzed P-wave spectra from 280 aftershocks of the 2015 Gorkha earthquake sequence ($4.0 \leq ML \leq 5.7$), recorded at 12 short-period stations. We performed the spectral inversion method using the reference site approach to isolate source, path and site terms from the recorded spectra. From the result of the inversion, we found out that the quality factor of P-wave (Qp) depends on frequency and fits well to the frequency-dependent Qp model ($Qp=90f^{0.7}$) in the frequency range up to 16 Hz. Displacement source spectra obtained after correcting frequency dependent path and site effects fairly follow the omega-squared source model over the entire magnitude range of analysis. By considering circular Brune-type source model, source parameters such as seismic moment, corner frequency, source radius and stress drop were estimated. The estimated stress drop values range from 2.1 to 95.4 MPa showing positive dependency on size of events. We also evaluated the spatial distribution of stress drop values and its relationship to co-seismic slip distribution during the mainshock. The result does not indicate any significant variation between stress drop of events in the large co-seismic slip area than those in the small slip area.

Keywords: Spectral inversion method, Q-factor, source parameters, Gorkha earthquake aftershocks.

1. INTRODUCTION

Owing to its location in the central part of the southwardly convex Himalayan arc, one of the most tectonically active zones on the earth, Nepal has experienced several destructive earthquakes throughout history. On 25 April 2015, an earthquake of Mw 7.8 occurred along the Himalayan front in the central part of the Nepal. The epicenter was located in the Gorkha district, about 80 km northwest from the capital city, Kathmandu. Numerous aftershock events recorded by the local seismic network of Nepal provide useful dataset for studying the detailed spectral characteristics of small to moderate earthquakes that occurred in and around the rupture zone of the mainshock. In this study, by using spectral inversion method (Andrews, 1986), we focus on separating the three main components: source, path and site terms of the observed ground motion in the frequency domain. Then, using the obtained source spectra, we estimate source parameters such as seismic moment, corner frequency and stress drop of the moderate aftershocks in order to understand the scaling relation between them.

2. DATA

In this study, velocity waveforms from aftershocks ($4 \leq ML \leq 5.7$) of the 2015 Gorkha earthquake sequence recorded at 12 short-period stations were used (Figure 1). Primary data processing of P-wave recordings from the vertical component is done using the SAC program. For computing the observed

*Department of Mines and Geology (DMG), Nepal.
**Assist. Professor, Disaster Prevention Research Institute, Kyoto University, Japan.
***International Institute of Seismology and Earthquake Engineering, Building Research Institute, Japan.

spectra, first, all the selected waveforms were corrected for the respective instrument response. Displacement Fourier spectra were then calculated for the 2.56 second P-wave windows, selected immediately after the arrival. In order to remove the noisy data, noise window is selected from 3.56 to 1 second (2.56 s) preceding the P-wave arrival. Prerequisites of FFT, such as removal of mean and linear trend, and 5% cosine taper are applied to both the P-wave and noise waveform.

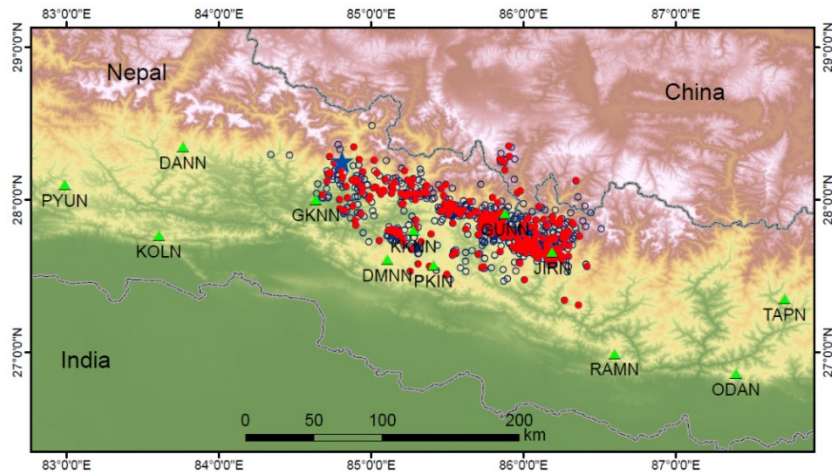

Figure 1. Map showing aftershock distribution of the 2015 Gorkha earthquake sequence. The aftershocks with local magnitude of greater than 4, which were recorded within one year after the mainshock are shown by open circles (NSC, 2016). Blue star represents epicenter of the mainshock. Events shown by red circle are used for the spectral inversion analysis in this study. The green triangles represent location of seismic stations used in this study.

During the inversion process, we selected events based on three criteria; hypocentral distance, signal to noise ratio, and number of recordings. First, we removed the data recorded at more than 250 km from the source in order to avoid the contamination of P-wave reflected phases at greater distances. The second criterion is signal to noise ratio, i.e., the average ratio at each discrete frequency must be at least 3 for three separate bands of 1 to 5 Hz, 5 to 10 Hz, and 11 to 15 Hz. Finally, we selected the events that contained at least five recordings after the screenings. The resulting data consists of 1825 P-wave spectra from 280 events recorded at 12 stations (Figure 1).

3. METHODOLOGY

3.1. Separation of seismic source spectra

In the frequency domain, the observed ground motion at receiver j for source i (O_{ij}) can be expressed as the product of three factors:

$$O_{ij}(f) = S_i(f)\, P_{ij}(f)\, G_j(f), \tag{1}$$

where $S_i(f)$ is the source spectrum including near source attenuation, $P_{ij}(f)$ is the path effect and $G_j(f)$ is the site response by site amplification and near receiver attenuation. Iwata and Irikura (1988) separated these three factors by applying the generalized linear inversion technique. They assumed both geometrical spreading (R_{ij}^{-1}) and the frequency dependent quality factor of wave attenuation $Q(f)$ contribute the path effect. Then the Eq. (1) is modified as;

$$O_{ij}(f) = S_i(f) G_j(f) R_{ij}^{-1} \exp\left(\frac{-\pi f t_{ij}}{Q(f)}\right), \tag{2}$$

where t_{ij} is the travel time of the wave from source to site. By taking the natural logarithm to Eq. (2), we can obtain the simultaneous linear equation as;

$$lnS_i + lnG_j + \frac{-\pi f t_{ij}}{Q(f)} = ln\left[O_{ij}R_{ij}\right]. \quad (3)$$

This linear equation can be solved numerically using the iterative least-squares approach. However, this poses a problem of trade-off between the results because of the three free parameters to solve. To avoid this unconstrained degree of freedom due to numerous unknown parameters, a constraint must be given to one of them. In this study, we use the reference site approach by using site effect of 2 for all frequency range, considering only free surface amplification effect (Iwata and Irikura, 1988).

3.2. Source parameters determination

From the spectral shape of the earthquake source model proposed by Brune (1970), the far field displacement amplitude spectra *u* is given by;

$$u(f) = \frac{\Omega_0}{1+\left(\frac{f}{f_c}\right)^n}, \quad (4)$$

where Ω_0 is the spectral amplitudes of the source at lower frequencies, f_c is the corner frequency, n is the high-frequency falloff rate (n = 2 for omega-squared model, which is the most commonly used value).

For the circular fault model, the seismic moment (Brune, 1970), corner frequency (f_c) (Andrews, 1986), and stress drop ($\Delta\sigma$) (Eshelby, 1957; Madariaga, 1976) can be calculated using the source spectra, obtained from the inversion, by the following equations:

$$M_0 = \frac{4\pi\rho v^3}{R_{\theta\varphi}}\Omega_0, \quad (5)$$

$$f_c = \frac{1}{2\pi}\sqrt{\frac{A_0}{\Omega_0}}, \quad (6)$$

$$\Delta\sigma = \frac{M_0 f_c^3}{(0.42\beta)^3}, \quad (7)$$

where ρ is the density, v is the seismic velocity (either P wave or S wave according to the wave type used), $R_{\theta\varphi}$ is the radiation pattern, A_0 is the flat level of acceleration spectra in the higher frequency band and β is the shear wave velocity near the source.

4. RESULTS AND DISCUSSION

4.1. Result of spectral inversion

In this study, three stations, GKNN, KKNN and PKIN, were selected individually as possible reference sites, since these three stations recorded most of the events. Figure 2 shows the estimated quality factor of P-wave (*Qp*-value) as a function of frequency, using the reference sites assumption mentioned above. In all three cases, the estimated *Qp*-values clearly depend on frequency, being roughly propositional to $f^{0.7}$ in the frequency range up to 16 Hz with almost no dependency on reference site.

Figure 3 shows the P-wave source displacement spectra obtained from the inversion at the reference site PKIN. A systematic trend of peaks and troughs is observed between 10 and 16 Hz in all the spectra. Another common feature observed in these source terms was that, all spectra were relatively flat up to 6 Hz and decayed after that. This spectral fall-off of all events at the same frequency could have been caused by the improper site term estimations during the inversion.

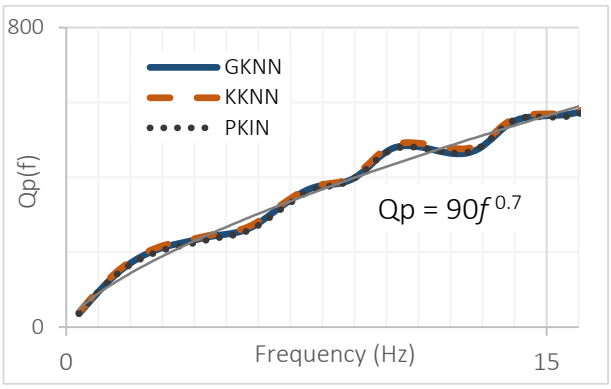

Figure 2. Estimated quality factor of P-wave from the inversion using three different reference sites.

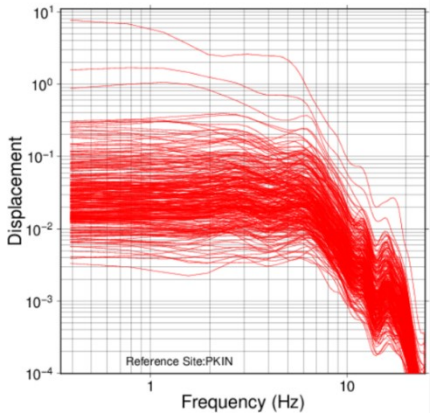

Figure 3. Displacement source spectra of all events obtained from inversion.

4.2. Correction of site term at the reference site

Some systematic features in the result of the inversion showed that the site terms were not properly removed from the observed spectra and we attempted to treat this issue using the method of Moya et al. (2000). According to this method, the site term for each event at the reference station PKIN, can be calculated by taking the ratio of source spectrum obtained from the inversion to the theoretical source spectrum for each corresponding spectrum (see Moya et al., 2000 for detail). To obtain the theoretical source spectra, we assumed that our source spectra follow omega-squared model and the displacement source spectra fall-off with the slope of -2 at a higher frequency range. Figure 4 shows the obtained average site term at the reference station (PKIN). Figure 5 shows the corrected displacement spectra after removing the site effect at the reference sites. The systematic peaks and troughs appeared in Figure 3 were significantly reduced.

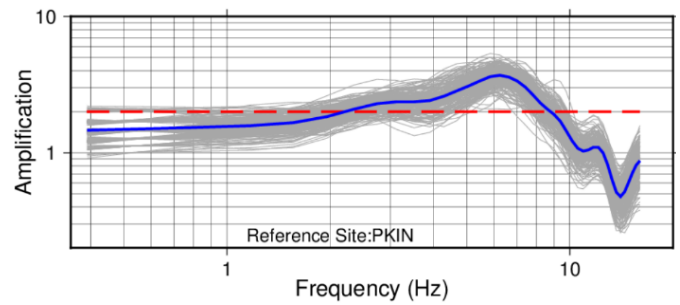

Figure 4. Average site response of reference (PKIN) station (blue line). Gray lines correspond to the site effects of the individual events. Red dashed line shows the initial assumption of constant amplification.

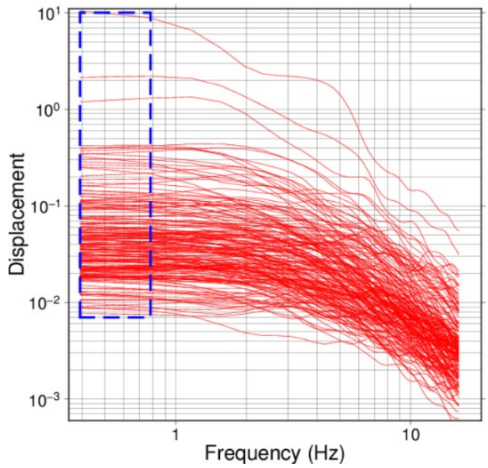

Figure 5. Corrected displacement source spectra of all events after removing the frequency dependent site response of the reference site.

4.3. Source parameter estimation

Seismic moment (M_0) values of all selected events were computed based on the Brune (1970) source model for circular faults, as given in Eq. (5). For the amplitude in the lower frequency part (Ω_0), we used the average of first two spectral points amplitudes (at 0.39 and 0.78 Hz) from in our final source spectra (Figure 5). We use the P-wave velocity V_p=5.6 km/sec, density ρ =2640 kg/m^3 and radiation pattern coefficient, $R_{\theta\varphi}$ = 0.52 (Boore and Boatwright, 1984). The corner frequencies for the source spectra were

determined using Eq. (6). For low-frequency displacement amplitude, amplitude value obtained for calculation of seismic moment were used, whereas for high-frequency acceleration amplitude the average of 16 samples above 10.16 Hz from calculated acceleration spectra was taken. Figure 6 shows the relationship between corner frequency and seismic moment. From the calculated seismic moments and the corner frequencies, the stress drop of events were computed by using the relation of Eshelby (1957) as given in Eq. (7). Estimated stress drop values ranged from 2.1 to 95.4 MPa, with large scatter in most magnitude ranges (Figure 7). However, for the entire range of data, there seems tendency of increasing stress drop with seismic moment.

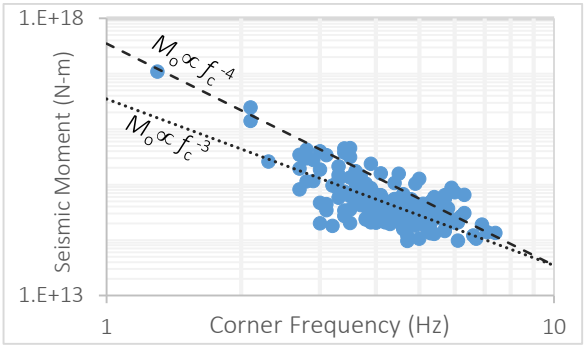

Figure 6. Seismic moment versus corner frequency for the earthquakes.

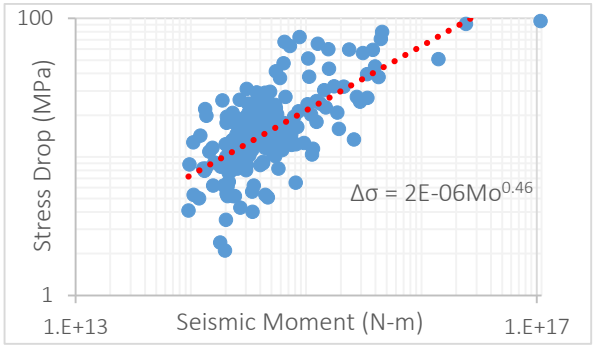

Figure 7. Seismic moment versus static stress drop.

4.4. Scaling Relations

As seen in Figure 6, smaller events (events with seismic moment less than 10^{15} N-m) generally adhered to $M_0 \propto f_c^{-3}$ accounting for the self-similarity between earthquakes. On the other hand, for larger events the relation of $M_0 \propto f_c^{-4}$ fitted better. Although we have smaller numbers of data for larger events, they seem not to scale with f_c^{-3}, which represents the constant stress drop model. The positive correlation between stress drop and magnitude in Figure 7 also supports this dependency.

However, as the stress drop is proportional to the third power of the corner frequency, small errors in the corner frequency of individual earthquakes led to a significant variation in the estimated stress drop. In order to obtain more stable corner frequencies, we stacked all the events within a bin of 0.1 Mw for the range of 3.3 to 4.4, where multiple events were available. Computed stacked spectra and corresponding corner frequencies are shown in Figure 8, with the slopes of constant stress drop. From the slope of obtained corner frequencies, it also showed that these earthquakes deviated from the self-similarity of constant stress drop within this magnitude range.

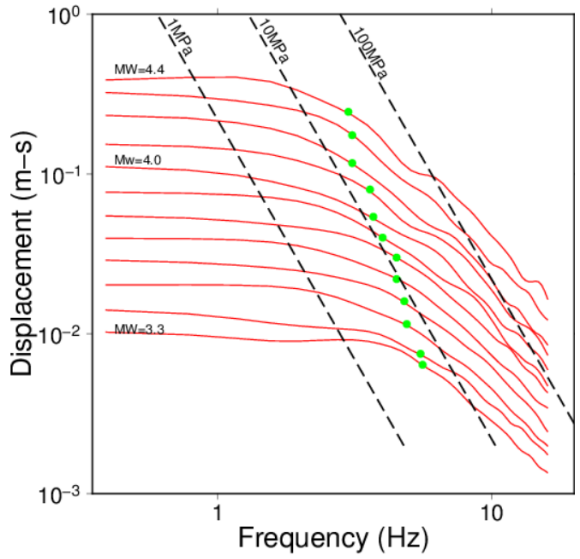

Figure 8. Stacked source spectra, binned in increments of 0.1 in estimated moment magnitude. The green points represent corner frequency of each stacked spectra.

4.5. Stress drops of aftershocks and slip distribution of the mainshock

We attempted to analyze spatial relation of mainshock slip area and static stress drop of the aftershocks. Figure 9 shows the stress drop values versus the co-

seismic slip, for the events that occurred within the slip area of the mainshock. We plotted events in three magnitude ranges considering the dependency of stress drop on the size of earthquakes. From this figure, we can observe that the larger events (Mw ≥ 4.1) were mostly occurred in the low slip area. For the middle ranged (3.7 ≤ Mw ≤ 4.0) events, there was large scatter in the stress drop values, however, aftershocks in the large slip area showed similar stress drop to the events in the low slip area. For the smaller events, we observed almost constant stress drop values throughout the slip area of the mainshock.

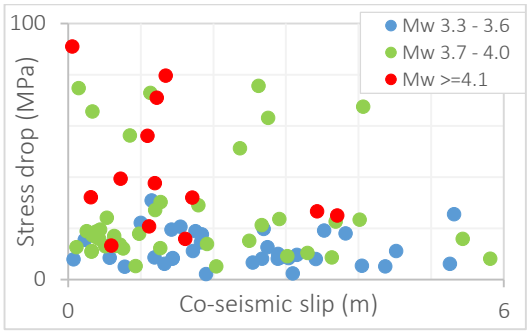

Figure 9. plot of static stress drop of aftershock to the co-seismic slip (Galetzka et al., 2015) of the mainshock.

5. CONCLUSIONS

In this study, we performed spectral inversion analysis in order to understand the source properties of the 2015 Gorkha earthquake sequences. We used P-wave spectra from 280 aftershocks (4.0 ≤ ML ≤ 5.7) recorded at the permanent seismic network of Nepal within one-year after the mainshock, with hypocentral distances up to 250 km. The spectral inversion was performed using the reference site approach to separate source, path and site terms from the recorded displacement spectra of 12 stations.

From the inversion results, we found out that the quality factor of P-wave (Qp) depends on frequency and values are proportional to $f^{0.7}$ in the frequency range up to 16 Hz. Displacement source spectra were obtained after removing the frequency dependent path and site effects. These spectra follow the omega-squared source model over the entire magnitude range of analysis. Source parameters such as seismic moment, corner frequency and stress drop of the aftershock events were obtained based on the Brune (1970) source model for circular fault. We obtained positive dependency of stress drop on the size of the events in the dataset. Comparison of stress drop values of aftershocks with the co-seismic slip of the mainshock did not show significant variation between stress drop of events in the large co-seismic slip area than those in the small slip area.

ACKNOWLEDGEMENTS

I would like to express my sincere gratitude to Masumi YAMADA, Toshiaki YOKOI, and Takumi HAYASHIDA for their continuous support, valuable suggestion and instruction during my study. I would also like to extend this gratitude to JICA, DMG, IISEE and GRIPS for providing the opportunity to enroll in this course.

REFERENCES

Andrews, D. J., 1986, Geophys. Monogr. Ser., 37, 259– 267.
Boore, D. M., and Boatwright, J., 1984, Bull. Seis. Soc. Am., 74, 1615–1621.
Brune, J. N., 1970, J. Geophys. Res., 75, 4997–5009.
Eshelby, J., 1957, Proc. R. Soc. London, Ser. A, 241, 376–396.
Galetzka, J., Melgar, D., Genrich, J.G. et al., 2015 Science 349, 1091–1095.
Iwata, T., and Irikura, K., 1988, Journal of Physics of the Earth, 36(4), 155-184.
Madariaga, R., 1976, Bull. Seis. Soc. Am., 66, 639–666.
Moya A, Aguirre, J., Irikura, K., 2000, Bull. Seis. Soc. Am., 90(4), 977–992.
Website: National Seismological Center (NSC), DMG, Nepal, http://www.seismonepal.gov.np.